J. Fluid Mech. (1973), *vol.* 58, *part* 1, *pp.* 39–51
Printed in Great Britain

Nonlinear stability of a liquid film adjacent to a supersonic stream

By ALI HASAN NAYFEH

Engineering Science and Mechanics Department, Virginia Polytechnic Institute and State University, Blacksburg, Virginia

AND WILLIAM S. SARIC

Sandia Laboratories, Albuquerque, New Mexico

(Received 28 July 1972)

The nonlinear stability of a liquid film adjacent to a supersonic gas stream is investigated. The gas is assumed to exert a mean shear stress at the liquid/gas interface which in turn establishes a linear mean velocity profile in the liquid. The analysis takes into account the pressure perturbation exerted by the gas on the liquid assuming the disturbed gas motion to be inviscid and the mean gas velocity profile to be uniform. The problem is formulated within the long wave approximation, and solutions are obtained for finite amplitude waves by using the method of multiple scales. The results predict the existence of finite amplitude periodic waves, in qualitative agreement with recent experimental observations.

1. Introduction

Recently, the equilibrium of the interface separating a liquid film from a supersonic stream received considerable attention. This attention has been motivated in part by the problems of transpiration cooling and cross-hatched ablation on re-entry vehicles. Of particular importance in transpiration cooling is the estimation of the liquid removal by either entrainment or evaporation. To estimate the amount of liquid entrained by the gas, we need to determine the stability characteristics of the liquid/gas interface. To estimate the amount of liquid removal by evaporation, we need to know the roughness characteristics of the interface, that is, the interface wave characteristics such as the wavelength and amplitude. The present paper analyses the stability of the interface as well as the characteristics of any waves which might exist on this interface.

The motion of the gas parallel to the liquid layer produces two important effects on the liquid. The first is the exertion of a mean shear stress at the liquid/gas interface which in turn establishes a mean velocity profile in the liquid. The second is the exertion of pressure and shear stress perturbations on the liquid due to the appearance of waves on the interface. In this paper, we investigate the effect of the pressure perturbation (Kelvin–Helmholtz mechanism) on the stability of a liquid film having a linear mean velocity profile.

Chang & Russell (1965) extended the classical Kelvin–Helmholtz model of two parallel, incompressible, inviscid streams by including compressibility in one fluid and viscosity in the other. They found that a liquid adjacent to a supersonic

stream is much more unstable than a liquid adjacent to a subsonic stream. In the subsonic case, the pressure perturbation is in anti-phase with the wave, while in the supersonic case, the pressure is in phase with wave slope, thus transferring the maximum energy to the interface. Nachtsheim (1970) extended the supersonic case of Chang & Russell by including the mean liquid velocity profile. Nayfeh & Saric (1971*b*) extended the work of Nachtsheim by including the effects of an arbitrary body force and a subsonic external flow; they also showed that a liquid layer adjacent to a supersonic stream is much more unstable than a liquid layer adjacent to a subsonic stream. Grabow & White (1972) extended the analysis of Nayfeh & Saric (1971*b*) by including the effect of a non-uniform gas flow.

These linear results are in disagreement with the experimental observations of Gater & L'Ecuyer (1969), Saric & Marshall (1971), Gold, Otis & Schlier (1971), Marshall (1971), Saric, Nayfeh & Bordner (1973) and Gold (1973). In the experiments of Gater & L'Ecuyer, the gas was nearly incompressible and turbulent, and the liquid layer was found to be unstable, the liquid drops entrained by the gas being observed. Gater & L'Ecuyer correlated the mass entrained with the entrainment group $(q)^{\frac{1}{2}}/\sigma$, where q is the dynamic pressure of the gas and σ is the surface tension of the liquid. Gold and co-workers (1971, 1973) and Saric *et al.* (1973) maintained the same range of the entrainment group as Gater & L'Ecuyer but at supersonic speeds. They did not observe any entrainment. In fact, they found that the ratio of the r.m.s. wave amplitude to the mean thickness of the liquid layer decreases as the surface pressure increases. This implies that increasing the entrainment group is stabilizing, in contrast with the subsonic experiments. In the experiments of Saric & Marshall (1971) and Marshall (1971), the gas motion was laminar and supersonic, and stable waves without entrainment were observed. Marshall (1971) measured the instantaneous depth of the liquid film by using an 'end-effect' capacitance gauge. Using this data we calculated the ratio of the r.m.s. wave amplitude to the mean depth, and found that this ratio decreases as the shear increases.

These experimental observations can be explained qualitatively by using the nonlinear theory of Nayfeh & Saric (1971*a*). They analysed the nonlinear stability of a quiescent viscous liquid film parallel to an inviscid compressible gas. In the subsonic case, they found that unstable linear disturbances continue to be unstable in the nonlinear case; thus conditions exist for liquid entrainment by the gas, in qualitative agreement with the experiments of Gater & L'Ecuyer. In the supersonic case, they found that stable linear disturbances are damped faster while unstable linear disturbances do not grow indefinitely but become steady periodic waves. Thus conditions for entrainment do not exist in this case, in qualitative agreement with the experiments of Gold and Saric and their co-workers. However, the analytical results are limited because the model neglects all the viscous effects of the gas. In particular, it neglects the mean shear stress exerted by the gas on the liquid which in turn implies neglect of the mean liquid velocity profile. Moreover, it neglects the shear perturbations as well as the effects of the gas velocity profile. In this paper, we remove the initial quiescent-liquid assumption by taking the liquid velocity profile (i.e. the mean shear stress exerted by the gas on the interface) into account.

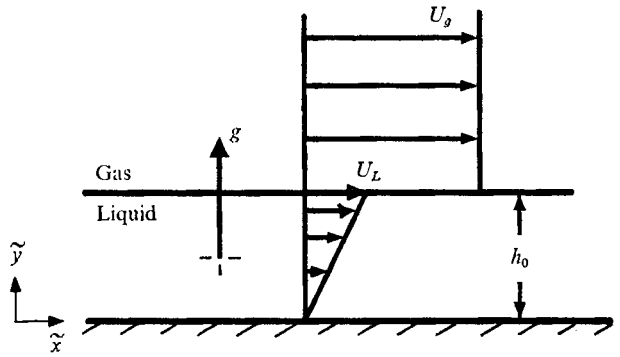

FIGURE 1. Geometry of the mean flow.

2. Problem formulation

The liquid layer is assumed to be thin with one side adjacent to a solid boundary and the other side adjacent to a parallel gas stream. As was mentioned in the introduction, the gas has two important effects on the liquid. The first is the establishment of a velocity profile in the liquid due to the exertion of a mean shear stress at the gas/liquid interface. The second is the production of pressure and shear perturbations, due to the presence of waves on the interface. In this paper, we study the effects of the liquid velocity profile as well as the pressure perturbation on the stability of the interface. The mean shear stress is calculated from the laminar or turbulent compressible flow past a flat plate, while the pressure perturbation is calculated from an inviscid uniform compressible flow past a wavy wall. This model therefore neglects the shear perturbation and the effect of the gas mean velocity gradient on the pressure perturbation. A discussion of this model is given in § 5.

A Cartesian co-ordinate system is introduced such that the $\tilde{x}$ axis lies in the liquid/solid interface and the $\tilde{y}$ axis is normal to this interface and directed toward the liquid as shown in figure 1. The liquid motion is governed by the following equations:

$$\tilde{u}_{\tilde{x}} + \tilde{v}_{\tilde{y}} = 0 \tag{2.1}$$

$$\tilde{u}_{\tilde{t}} + \tilde{u}\tilde{u}_{\tilde{x}} + \tilde{v}\tilde{u}_{\tilde{y}} = -\rho^{-1}\tilde{p}_{\tilde{x}} + \nu(\tilde{u}_{\tilde{x}\tilde{x}} + \tilde{u}_{\tilde{y}\tilde{y}}), \tag{2.2}$$

$$\tilde{v}_{\tilde{t}} + \tilde{u}\tilde{v}_{\tilde{x}} + \tilde{v}\tilde{v}_{\tilde{y}} = -\rho^{-1}\tilde{p}_{\tilde{y}} + g + \nu(\tilde{v}_{\tilde{x}\tilde{x}} + \tilde{v}_{\tilde{y}\tilde{y}}), \tag{2.3}$$

where ν, ρ and $\tilde{p}$ are the liquid kinematic viscosity, density and pressure, respectively, $\tilde{u}$ and $\tilde{v}$ are the velocities along the $\tilde{x}$ and $\tilde{y}$ axes and g is the body force per unit mass directed from the liquid to the gas.

We assume that, in the steady-state case, the gas exerts a shear stress τ_0 on the gas/liquid interface, where

$$\tau_0 = c_f \rho_g U_g^2, \tag{2.4}$$

with c_f the coefficient of friction and the subscript g referring to the gas properties. Using the continuity of shear and pressure conditions at the undisturbed liquid/gas interface, we find the following laminar steady-state solution in the liquid layer:

$$\tilde{U} = (\tau_0/\rho\nu)\,\tilde{y}, \quad \tilde{P} = -\rho g(h_0 - \tilde{y}) + \tilde{P}_0, \tag{2.5}$$

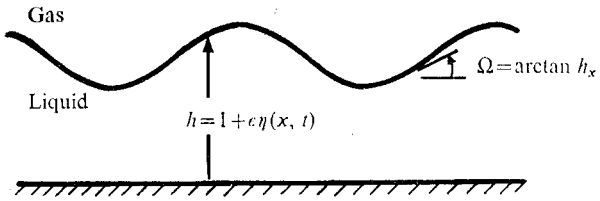

FIGURE 2. Geometry of wave motion.

where $\tilde{P}_0$ is the gas pressure and h_0 is the undisturbed liquid depth. From (2.5), the liquid velocity at the interface is

$$U_L = \tau_0 h_0/\rho\nu. \tag{2.6}$$

To study the stability of this steady-state configuration, we subject it to finite amplitude disturbances. Moreover, we introduce dimensionless variables according to

$$\left.\begin{aligned} x = \tilde{x}\alpha/h_0 \quad y = \tilde{y}/h_0, \quad \alpha = h_0/l, \quad h = \tilde{h}/h_0, \\ U = \tilde{U}/U_L, \quad u + U = \tilde{u}/U_L, \quad v = \tilde{v}/\alpha U_L, \\ t = \tilde{t}\alpha U_L/h_0, \quad p = \tilde{P}/\rho U_L^2, \quad p + P = \tilde{p}/\rho U_L^2, \end{aligned}\right\} \tag{2.7}$$

where u and v are the liquid disturbance velocities, p is the liquid disturbance pressure, l is a characteristic length (e.g. the wavelength of an initially sinusoidal disturbance), $\tilde{h}$ is the height of the disturbed interface and α is a dimensionless wavenumber. Substituting (2.7) into (2.1)–(2.3) and using (2.5) and (2.6), we obtain equations governing u, v and p. By introducing the stream function $\psi(x, y, t)$ defined by

$$(u, v) = (\psi_y, -\psi_x) \tag{2.8}$$

we combine the liquid disturbance equations into

$$\begin{aligned} \psi_{yyyy} = \alpha R[\psi_{yyt} + (y + \psi_y)\psi_{xyy} - \psi_{yyy}\psi_x] \\ - 2\alpha^2\psi_{xxyy} + \alpha^3 R[\psi_{xxt} + (y + \psi_y)\psi_{xxx} - \psi_x\psi_{xxy}] - \alpha^4\psi_{xxxx}, \end{aligned} \tag{2.9}$$

where

$$R = U_L h_0/\nu\text{: the liquid-layer Reynolds number.} \tag{2.10}$$

Since the shear perturbation and gas mean velocity gradients are neglected in our model, the disturbed gas motion can be represented by the potential function $U_g l\Phi(x, Y, t)$, where the dimensionless function Φ is given by

$$\begin{aligned} \Phi_{YY} - m^2\Phi_{xx} = M^2[\tfrac{1}{2}(\gamma - 1)(2\Phi_x + \Phi_x^2 + \Phi_Y^2)(\Phi_{xx} + \Phi_{YY}) + (2\Phi_x + \Phi_x^2)\Phi_{xx} \\ + 2(1 + \Phi_x)\Phi_Y\Phi_{xY} + \Phi_Y^2\Phi_{YY}], \quad -\infty < x < \infty, \ \alpha(h - 1) \leqslant Y < \infty. \end{aligned} \tag{2.11}$$

Here, $h(x, t)$ is the dimensionless height of the disturbed interface shown in figure 2, M is the Mach number, γ is the ratio of the gas specific heats,

$$Y = (\tilde{y} - h_0)/l \quad \text{and} \quad m^2 = M^2 - 1.$$

In (2.11) and subsequent boundary conditions, we assume that the gas velocity is very much larger than the phase velocity so that the transient motion of the gas can be neglected.

The stability problem is completed by a specification of the boundary conditions. At the solid/liquid interface, the liquid velocity components u and v vanish; that is

$$\psi_y(x, 0, t) = \psi(x, 0, t) = 0. \tag{2.12}$$

Away from the gas/liquid interface, the gas disturbance vanishes upstream:

$$\Phi(x, Y, t) = 0 \quad \text{upstream.} \tag{2.13}$$

The conditions that the normal velocity is continuous across the interface and that the fluids move with the interface give the kinematic conditions

$$h_t + (h + \psi_y) h_x + \psi_x = 0 \quad \text{at} \quad y = h, \tag{2.14}$$

$$\alpha h_x - \Phi_Y + \alpha h_x \Phi_x = 0 \quad \text{at} \quad Y = \alpha(h-1). \tag{2.15}$$

With the neglect of the shear perturbation exerted by the gas on the disturbed gas/liquid interface, the continuity of tangential stresses across this interface demands that

$$(\psi_{yy} - \alpha^2 \psi_{xx})(1 - \alpha^2 h_x^2) - 4\alpha^2 \psi_{xy} h_x = 0 \quad \text{at} \quad y = h. \tag{2.16}$$

The continuity of normal stresses across the liquid/gas interface demands that

$$p + G(h-1) + \frac{2\alpha}{R} \psi_{xy} \frac{1 - \alpha^2 h_x^2}{1 + \alpha^2 h_x^2} + T \frac{h_{xx}}{(1 + \alpha^2 h_x^2)^{\frac{3}{2}}}$$

$$+ \frac{2\alpha}{R} (\psi_{yy} - \alpha^2 \psi_{xx}) \frac{h_x}{1 + \alpha^2 h_x^2} = \frac{m}{2\alpha^2 R} \chi C_p \quad \text{at} \quad y = h, \quad Y = \alpha(h-1), \tag{2.17}$$

where

$$\chi = \alpha^2 R \rho_g U_g^2 / \rho U_L^2 m = \alpha^2 / c_f (M^2 - 1)^{\frac{1}{2}}, \tag{2.18}$$

$$T = \sigma h_0 / \rho U_L^2 l^2, \quad G = g h_0 / U_L^2, \tag{2.19}$$

$$C_p = \frac{2}{\gamma M^2} \left\{ \left[1 - \frac{\gamma - 1}{2} M^2 (2\Phi_x + \Phi_x^2 + \Phi_Y^2) \right]^{\gamma/(\gamma-1)} - 1 \right\}, \tag{2.20}$$

with σ the liquid surface tension, C_p the gas pressure perturbation coefficient, and T and G the reciprocal Weber and Froude numbers respectively. The liquid pressure p is eliminated from (2.17) by using the x-momentum equation

$$p_x = \frac{1}{\alpha R} \psi_{yyy} - [\psi_{yt} + (y + \psi_y) \psi_{xy} - (1 + \psi_{yy}) \psi_x] + \frac{\alpha}{R} \psi_{xxy}. \tag{2.21}$$

3. Solution for long waves

A perturbation solution is sought for the case of a disturbance whose length scale l is large compared with the thickness h_0; that is, $\alpha = h_0/l$ is small. For an initially sinusoidal disturbance with wavelength λ, $\alpha = 2\pi h_0/\lambda$. To accomplish this, we determine expansions for ψ and Φ from (2.9)–(2.13) and (2.15)–(2.21) and substitute the resulting expansion for ψ in (2.14) to obtain an equation for $h(x, t)$. We assume expansions of the form

$$\psi = \psi_0 + \alpha \psi_1 + \ldots, \quad p = \alpha^{-1} p_{-1} + p_0 + \ldots, \quad \Phi = \alpha \Phi_1 + \alpha^2 \Phi_2 + \ldots, \tag{3.1}$$

in (2.9), (2.11) and (2.12)–(2.20), equate coefficients of like powers of α and obtain the following:

First-order problem

$$\psi_{0yyyy} = 0, \quad \psi_0 = \psi_{0y} = 0 \quad \text{at} \quad y = 0, \quad \psi_{0yy} = 0 \quad \text{at} \quad y = h, \quad (3.2), (3.3), (3.4)$$

$$p_{-1}(x, h, t) = -(\chi m/R)\,\Phi_{1x}(x, 0, t) \quad \text{at} \quad y = h, \quad (3.5)$$

$$p_{-1x} = R^{-1}\psi_{0yyy}, \quad \Phi_{1YY} - m^2\Phi_{1xx} = 0, \quad (3.6), (3.7)$$

$$\Phi_1 = 0 \quad \text{upstream}, \quad \Phi_{1Y} = h_x \quad \text{at} \quad Y = 0. \quad (3.8), (3.9)$$

Second-order problem

$$\psi_{1yyyy} = R[\psi_{0yyt} + (y + \psi_{0y})\,\psi_{0xyy} - \psi_{0yyy}\psi_{0x}], \quad (3.10)$$

$$\psi_1 = \psi_{1y} = 0 \quad \text{at} \quad y = 0, \qquad \psi_{1yy} = 0 \quad \text{at} \quad y = h_0 \quad (3.11), (3.12)$$

$$p_0 = -G(h-1) - Th_{xx} - (\chi m/R)\,[\Phi_{2x} - \tfrac{1}{2}m^2\Phi_{1x}^2 + \tfrac{1}{2}\Phi_{1Y}^2 + (h-1)\,\Phi_{1xY}]$$
$$\text{at} \quad y = h, \; Y = 0, \quad (3.13)$$

$$p_{0x} = R^{-1}\psi_{1yyy} - [\psi_{0yt} + (y + \psi_{0y})\,\psi_{0xy} - (1 + \psi_{0yy})\,\psi_{0x}], \quad (3.14)$$

$$\Phi_{2YY} - m^2\Phi_{2xx} = M^2[(\gamma+1)\,\Phi_{1x}\Phi_{1xx} + (\gamma-1)\,\Phi_{1x}\Phi_{1YY} + 2\Phi_{1Y}\Phi_{1xY}], \quad (3.15)$$

$$\Phi_2 = 0 \text{ upstream}, \quad (3.16)$$

$$\Phi_{2Y} = h_x\Phi_{1x} - (h-1)\,\Phi_{1YY} \quad \text{at} \quad Y = 0. \quad (3.17)$$

The solution of (3.2)–(3.6) is

$$\psi_0 = a_2 y^2 + a_3 y^3, \quad (3.18)$$

where
$$a_3 = -\tfrac{1}{6}\chi m\Phi_{1xx}(x, 0, t), \quad a_2 = -3ha_3. \quad (3.19)$$

Substituting for ψ_0 into (3.10) and solving the resulting equation subject to the boundary conditions (3.11)–(3.14), we get

$$\psi_1 = R[b_2 y^2 + b_3 y^3 + \tfrac{1}{12}b_4 y^4 + \tfrac{1}{60}b_5 y^5 + \tfrac{1}{60}b_6 y^6 + \tfrac{1}{70}b_7 y^7], \quad (3.20)$$

where

$$b_3 = -\tfrac{1}{6}\{Gh_x + Th_{xxx} + (\chi m/R)\,[\Phi_{2xx} - m^2\Phi_{1x}\Phi_{1xx} + \Phi_{1Y}\Phi_{1xY} + h_x\Phi_{1xY}$$
$$+ (h-1)\,\Phi_{1xxY}]\} \quad \text{at} \quad Y = 0,$$

$$b_4 = a_{2t}, \quad b_5 = 3a_{3t} + (1 + 2a_2)\,a_{2x}, \quad b_6 = (1 + 2a_2)\,a_{3x}, \quad b_7 = a_3 a_{3x},$$
$$b_2 = -3b_3 h - \tfrac{1}{2}b_4 h^2 - \tfrac{1}{6}b_5 h^3 - \tfrac{1}{4}b_6 h^4 - \tfrac{3}{10}b_7 h^5. \quad (3.21)$$

Since
$$\partial[\psi(x, h)]/\partial x = \psi_x(x, y)|_{y=h} + \psi_y(x, y)\,h_x|_{y=h},$$

the boundary condition (2.14) gives

$$h_t + hh_x + (\partial/\partial x)\,[\psi_0(x, h) + \alpha\psi_1(x, h)] + O(\alpha^2) = 0. \quad (3.22)$$

Substituting for ψ_0 and ψ_1 into (3.22) gives

$$h_t + hh_x - (\partial/\partial x)\{2a_3 h^3 + \alpha R[2b_3 h^3 + \tfrac{5}{12}a_{2t}h^4 + \tfrac{3}{20}(3a_{3t} + (1 + 2a_2)\,a_{2x}h^5$$
$$+ \tfrac{7}{30}(1 + 2a_2)\,a_{3x}h^6 + \tfrac{2}{7}a_3 a_{3x}h^7]\} + O(\alpha^2) = 0. \quad (3.23)$$

Although (3.23) is valid for long wavelengths only, it is valid for all shapes and amplitudes of disturbances. To simplify this equation, we let

$$h(x, t) = 1 + \epsilon\eta(x, t), \quad (3.24)$$

where ϵ is a small but finite dimensionless quantity. With this assumption, (3.23) becomes

$$\begin{aligned}
&\eta_t+\eta_x+\tfrac{1}{3}\chi m\phi_{1xxx}+\epsilon[\eta\eta_x+\chi m(\eta\phi_{1xx})_x]+\epsilon^2\chi m(\eta^2\phi_{1xx})_x\\
&\quad+\tfrac{1}{3}\epsilon^3[\chi m(\eta^3\phi_{1xx})_x+\tilde{\alpha}R(G\eta_{xx}+T\eta_{xxxx}-\tfrac{2}{5}\chi m\phi_{1xxxt}-\tfrac{13}{120}\chi m\phi_{1xxxx})]\\
&\quad+\tfrac{1}{3}\epsilon^4\tilde{\alpha}\chi m(\partial/\partial x)(\phi_{2xx}-m^2\phi_{1x}\phi_{1xx}+\phi_{1Y}\phi_{1xY}+\eta_x\phi_{1xY}+\eta\phi_{1xxY})\\
&\quad+\epsilon^4\tilde{\alpha}R(\partial/\partial x)[\eta(G\eta_x+T\eta_{xxx}-\tfrac{13}{60}\chi m\phi_{1xxx}-\tfrac{2}{3}\chi m\phi_{1xxt})-\tfrac{5}{24}\chi m\phi_{1xx}\eta_t\\
&\quad-\tfrac{3}{40}\chi m\phi_{1xx}\eta_x-\tfrac{37}{840}\chi^2m^2\phi_{1xx}\phi_{1xxx}]+\epsilon^5\tilde{\alpha}\chi m(\partial/\partial x)[\eta(\phi_{2xx}-m^2\phi_{1x}\phi_{1xx}\\
&\quad+\phi_{1Y}\phi_{1xY}+\eta_x\phi_{1xY}+\eta\phi_{1xxY})]+\epsilon^5\tilde{\alpha}R(\partial/\partial x)[\eta^2(G\eta_x+T\eta_{xxx}-\tfrac{4}{3}\chi m\phi_{1xxt}\\
&\quad-\tfrac{13}{24}\chi m\phi_{1xxx})-\tfrac{5}{6}\chi m\eta\eta_t\phi_{1xx}-\tfrac{3}{8}\chi m\eta\eta_x\phi_{1xx}-\tfrac{37}{120}\chi^2m^2\eta\phi_{1xx}\phi_{1xxx}\\
&\quad-\tfrac{3}{40}\chi^2m^2\eta_x\phi_{1xx}\phi_{1xx}]+O(\epsilon^6)=0, \qquad (3.25)
\end{aligned}$$

where
$$\Phi_1=\epsilon\phi_1,\quad \phi_1=O(1), \qquad (3.26)$$
$$\Phi_2=\epsilon^2\phi_2,\quad \phi_2=O(1) \qquad (3.27)$$
and
$$\alpha=\epsilon^3\tilde{\alpha},\quad \tilde{\alpha}=O(1). \qquad (3.28)$$

In the next section, we consider the case of an initially sinusoidal disturbance.

4. Initially sinusoidal case

To find an approximate solution to (3.25) subject to an initially sinusoidal disturbance, we Fourier analyse the wave amplitude function η by letting

$$\epsilon\eta(x,t)=\sum_{n=1}^{\infty}\epsilon^n[\eta_n(t)\,e^{inx}+\bar{\eta}_n(t)\,e^{-inx}]. \qquad (4.1)$$

Then the solution of (3.7)–(3.9) is

$$\epsilon\phi_1=-\frac{1}{m}\sum_{n=1}^{\infty}\epsilon^n[\eta_n(t)\,e^{in(x-mY)}+\bar{\eta}_n(t)\,e^{-in(x-mY)}]. \qquad (4.2)$$

The solution of (3.15)–(3.17) which will affect the solution of η to the order indicated in (3.25) is

$$\begin{aligned}
\phi_2=&\frac{i}{2m^2}\left[1-m^2-\frac{M^4(\gamma+1)}{4m^2}\right]\eta_1^2\,e^{2i(x-mY)}\\
&-\frac{i\epsilon}{m^2}\left[4+5m^2-\frac{M^4(\gamma+1)}{m^2}\right]\bar{\eta}_1\eta_2e^{i(x-mY)}+\ldots. \qquad (4.3)
\end{aligned}$$

By substituting (4.1)–(4.3) into (3.25) and equating the coefficient of each harmonic of x to zero, we get

$$\begin{aligned}
&\frac{d\eta_1}{dt}+i(1+\tfrac{1}{3}\chi)\eta_1+i\epsilon^2[(1+5\chi)\bar{\eta}_1\eta_2+3\chi\eta_1^2\bar{\eta}_1]+\tfrac{1}{3}\epsilon^3\tilde{\alpha}R\left[(T-G+\tfrac{13}{120}\chi)]\eta_1\right.\\
&\quad\left.-\tfrac{2}{5}i\chi\frac{d\eta_1}{dt}\right]+i\epsilon^4[(1+13\chi)\bar{\eta}_2\eta_3+\chi(18\eta_1\eta_2\bar{\eta}_2+11\bar{\eta}_1^2\eta_3)+\tfrac{7}{3}\chi(3\eta_1\bar{\eta}_1^2\eta_2+\eta_1^3\eta_2)]\\
&\quad+\epsilon^5\tilde{\alpha}\frac{\chi}{m}\left[1-\frac{M^4(\gamma+1)}{4m^2}\right](2\eta_1^2\bar{\eta}_1-\tfrac{4}{3}\bar{\eta}_1\eta_2)+\epsilon^5\tilde{\alpha}R\left[(7T-G+\tfrac{41}{30}\chi+\tfrac{37}{210}\chi^2)\bar{\eta}_1\eta_2\right.\\
&\quad-i\chi\left(\tfrac{3}{2}\eta_2\frac{d\bar{\eta}_1}{dt}+\tfrac{23}{8}\bar{\eta}_1\frac{d\eta_2}{dt}\right)+(T-G+\tfrac{11}{12}\chi+\tfrac{23}{60}\chi^2)\eta_1^2\bar{\eta}_1\\
&\quad\left.-\tfrac{13}{6}i\chi\left(2\eta_1\bar{\eta}_1\frac{d\eta_1}{dt}+\eta_1^2\frac{d\bar{\eta}_1}{dt}\right)\right]+O(\epsilon^6)=0, \qquad (4.4)
\end{aligned}$$

$$\frac{d\eta_2}{dt}+2i(1+\tfrac{4}{3}\chi)\eta_2+i(1+2\chi)\eta_1^2+i\epsilon^2[2(1+10\chi)\bar{\eta}_1\eta_3+24\chi\eta_1\bar{\eta}_1\eta_2+\tfrac{8}{3}\chi\eta_1^3\bar{\eta}_1]$$
$$+\frac{4}{3}\frac{\epsilon^3\tilde{\alpha}\chi}{m}\left[1-\frac{M^4(\gamma+1)}{4m^2}\right]\eta_1^2+\tfrac{1}{3}\epsilon^3\tilde{\alpha}R\left[4(4T-G+\tfrac{13}{30}\chi)\eta_2-\tfrac{16}{5}i\chi\frac{d\eta_2}{dt}\right.$$
$$\left.+6(T-G+\tfrac{7}{24}\chi+\tfrac{37}{840}\chi^2)\eta_1^2-\tfrac{21}{4}i\chi\eta_1\frac{d\eta_1}{dt}\right]+O(\epsilon^4)=0, \tag{4.5}$$

$$d\eta_3/dt+3i[(1+3\chi)\eta_3+(1+5\chi)\eta_1\eta_2+\chi\eta_1^3]+O(\epsilon^2)=0. \tag{4.6}$$

To obtain an appropriate solution to (4.4)–(4.6), we use the method of multiple scales (Nayfeh 1973) by letting

$$\eta_n(t)=\sum_{m=0}^{5}\epsilon^m\eta_{nm}(T_0,T_1,\ldots,T_5), \tag{4.7}$$

where

$$T_m=\epsilon^m t. \tag{4.8}$$

An alternative technique for obtaining the solution is presented in the appendix. Substituting (4.7) and (4.8) into (4.4)–(4.6) and equating coefficients of like powers of ϵ, we obtain equations for η_{nm}. The zeroth-order equations are

$$\partial\eta_{10}/\partial T_0+i(1+\tfrac{1}{3}\chi)\eta_{10}=0, \tag{4.9}$$

$$\partial\eta_{20}/\partial T_0+2i(1+\tfrac{4}{3}\chi)\eta_{20}=-i(1+2\chi)\eta_{10}^2, \tag{4.10}$$

$$\partial\eta_{30}/\partial T_0+3i(1+3\chi)\eta_{30}=-3i(1+5\chi)\eta_{10}\eta_{20}-3i\chi\eta_{10}^3. \tag{4.11}$$

The solution of (4.9) is

$$\eta_{10}=A_{10}(T_1,T_2,\ldots,T_5)\exp[-i(1+\tfrac{1}{3}\chi)T_0]. \tag{4.12}$$

Then the particular solutions of (4.10) and (4.11) are

$$\eta_{20}=-\frac{1+2\chi}{2\chi}A_{10}^2\exp[-2i(1+\tfrac{1}{3}\chi)T_0], \tag{4.13}$$

$$\eta_{30}=\frac{3}{16}\frac{1+7\chi+8\chi^2}{\chi^2}A_{10}^3\exp[-3i(1+\tfrac{1}{3}\chi)T_0]. \tag{4.14}$$

In these solutions, as well as in the higher order solutions, the solutions of the homogeneous equations are omitted.

The first-order problem becomes

$$\frac{\partial\eta_{11}}{\partial T_0}+i(1+\tfrac{1}{3}\chi)\eta_{11}=-\frac{\partial A_{10}}{\partial T_1}\exp[-i(1+\tfrac{1}{3}\chi)T_0]. \tag{4.15}$$

The particular solution of (4.15) contains a secular term of the form

$$T_0\exp[-i(1+\tfrac{1}{3}\chi)T_0],$$

which makes η_{11}/η_{10} unbounded as $T_0\to\infty$ unless

$$A_{10}=A_{11}(T_2,T_3,T_4,T_5).$$

Consequently,

$$\eta_{11}=\eta_{21}=\eta_{31}=0.$$

Proceeding to second order, we have

$$\frac{\partial \eta_{12}}{\partial T_0} + i(1+\tfrac{1}{3}\chi)\,\eta_{12} = -\frac{\partial \eta_{10}}{\partial T_2} - i(1+5\chi)\,\bar{\eta}_{10}\eta_{20} - 3i\chi\eta_{10}^2\bar{\eta}_{10}, \tag{4.16}$$

$$\frac{\partial \eta_{22}}{\partial T_0} + 2i(1+\tfrac{4}{3}\chi)\,\eta_{22} = -\frac{\partial \eta_{20}}{\partial T_2} - 2i(1+2\chi)\,\eta_{10}\eta_{12} - 2i(1+10\chi)\,\bar{\eta}_{10}\eta_{30} - 24i\chi\eta_{10}\bar{\eta}_{10}\eta_{20} - \tfrac{8}{3}i\chi\eta_{10}^3\bar{\eta}_{10}. \tag{4.17}$$

Substituting for η_{10} and η_{20} from (4.12) and (4.13) into (4.16), we obtain

$$\frac{\partial \eta_{12}}{\partial T_0} + i(1+\tfrac{1}{3}\chi)\,\eta_{12} = -\left(\frac{\partial A_{11}}{\partial T_2} - ic_2 A_{11}^2\bar{A}_{11}\right)\exp\left[-i(1+\tfrac{1}{3}\chi)\,T_0\right], \tag{4.18}$$

where

$$c_2 = (1+7\chi+4\chi^2)/2\chi. \tag{4.19}$$

Secular terms will be eliminated from η_{12} if

$$\partial A_{11}/\partial T_2 = ic_2 A_{11}\bar{A}_{11}A_{11}. \tag{4.20}$$

Then the particular solutions of (4.16) and (4.17) are

$$\eta_{12} = 0, \tag{4.21}$$

$$\eta_{22} = \frac{3-45\chi-198\chi^2-112\chi^3}{48\chi^3}\,A_{11}^3\bar{A}_{11}\exp\left[-2i(1+\tfrac{1}{3}\chi)\,T_0\right]. \tag{4.22}$$

The third-order problem is then

$$\frac{\partial \eta_{13}}{\partial T_0} + i(1+\tfrac{1}{3}\chi)\,\eta_{13} = -\left(\frac{\partial A_{11}}{\partial T_3} - c_3 A_{11}\right)\exp\left[-i(1+\tfrac{1}{3}\chi)\,T_0\right], \tag{4.23}$$

$$\frac{\partial \eta_{23}}{\partial T_0} + 2i(1+\tfrac{4}{3}\chi)\,\eta_{23} = -\frac{\partial \eta_{20}}{\partial T_3} - 2i(1+2\chi)\,\eta_{10}\eta_{13} - \frac{4\tilde{\alpha}\chi}{3m}\left(1-\frac{\gamma+1}{4m^2}M^4\right)\eta_{10}^2 - \tfrac{1}{3}\tilde{\alpha}R\left[4(4T-G+\tfrac{13}{30}\chi)\,\eta_{20} - \tfrac{16}{5}i\chi\frac{\partial \eta_{20}}{\partial T_0} + (6T-G+\tfrac{7}{24}\chi+\tfrac{37}{840}\chi^2)\,\eta_{10}^2 - \tfrac{21}{4}i\chi\eta_{10}\frac{\partial \eta_{10}}{\partial T_0}\right], \tag{4.24}$$

where

$$c_3 = -\tfrac{1}{3}\tilde{\alpha}R(T-G-\tfrac{7}{24}\chi-\tfrac{2}{15}\chi^2). \tag{4.25}$$

Secular terms will be eliminated from η_{13} if

$$\partial A_{11}/\partial T_3 = c_3 A_{11}. \tag{4.26}$$

Then the particular solutions of (4.23) and (4.24) are

$$\eta_{13} = 0, \tag{4.27}$$

$$\eta_{23} = \frac{i}{6\chi^2}\left\{4\tilde{\alpha}\frac{\chi^2}{m}\left(1-\frac{\gamma+1}{4m^2}M^4\right) + \tilde{\alpha}R[-(7+8\chi)\,T + (1-4\chi)\,G + \tfrac{49}{24}\chi + \tfrac{91}{60}\chi^2 + \tfrac{8}{21}\chi^3]\right\}A_{11}^2\exp\left[-2i(1+\tfrac{1}{3}\chi)\,T_0\right]. \tag{4.28}$$

Analysis of the fourth-order equations yields

$$\eta_{14} = 0, \quad \partial A_{11}/\partial T_4 = ic_4 A_{11}^2 \bar{A}_{11}^2 A_{11}, \tag{4.29}$$

where
$$c_4 = (1+86\chi+489\chi^2+752\chi^3+192\chi^4)/32\chi^3, \tag{4.30}$$

while analysis of the fifth-order equations gives

$$\eta_{15} = 0, \quad \partial A_{11}/\partial T_5 = c_5 A_{11} \bar{A}_{11} A_{11}, \tag{4.31}$$

where

$$c_5 = (\tilde{\alpha}R/6\chi^2)[-(7+22\chi+4\chi^2)T+(1-2\chi-20\chi^2)G + \tfrac{1}{30}(\tfrac{245}{4}\chi+\tfrac{321}{4}\chi^2-\tfrac{1755}{7}\chi^3-\tfrac{1072}{7}\chi^4)]. \tag{4.32}$$

Letting $A_{11} = \frac{1}{2}a\exp(i\beta)$ with real a and β, we find that $a = a(T_3, T_5)$ and

$$\partial a/\partial T_3 = c_3 a, \quad \partial a/\partial T_5 = \tfrac{1}{4}c_5 a^3.$$

Therefore,
$$da/dt = \epsilon^3(c_3+\tfrac{1}{4}\epsilon^2 c_5 a^2)a, \tag{4.33}$$

or
$$\frac{da}{dt} = -\tfrac{1}{3}\alpha R(T-G-\tfrac{7}{24}\chi-\tfrac{2}{15}\chi^2)a+\epsilon^2\frac{\alpha R}{24\chi^2}[-(7+22\chi+4\chi^2)T + (1-2\chi-20\chi^2)G+\tfrac{1}{120}(245\chi+321\chi^2)-\tfrac{1}{210}(1755\chi^3+1072\chi^4)]. \tag{4.34}$$

The stability of the interface depends on the signs and relative magnitudes of the coefficients c_3 and c_5. The linear motion is stable or unstable depending on whether c_3 is negative or positive definite, while the nonlinear motion is stabilizing or destabilizing depending on whether c_5 is negative or positive. Figure 3 shows the variation of c_3 and c_5 with the wavenumber α for specific liquid and gas flow conditions. The coefficient c_3 is negative and the linear motion is stable except in the interval $\alpha_2 \leqslant \alpha \leqslant \alpha_c$, where α_c is the upper neutrally stable wavenumber. The exact numerical solution of the linear problem shows that $\alpha_c \approx 3$; α_c is not shown in the figure because the long wave approximation is not valid for such an α. The coefficient c_5 is positive only for $\alpha_1 \leqslant \alpha \leqslant \alpha_3$. Thus, disturbances with wavenumbers less than α_1 decay to zero, while disturbances with $\alpha > \alpha_3$ become stable steady periodic waves with amplitude $a_s = (-4c_3/\epsilon^2 c_5)^{\frac{1}{2}}$, irrespective of their initial amplitudes. A disturbance with α in the interval $[\alpha_1, \alpha_2]$ is stable or unstable depending on whether its initial amplitude is less or greater than the amplitude $a_s = (-4c_3/\epsilon^2 c_5)^{\frac{1}{2}}$; a disturbance with this amplitude is an unstable periodic wave. Finally, all disturbances with α in the interval $[\alpha_2, \alpha_3]$ are unstable irrespective of their initial amplitudes.

It should be mentioned that it is possible to have situations in which $\alpha_3 < \alpha_2$ and situations in which c_5 is negative for all α. However, in all liquid and gas flow conditions, the present analysis predicts a range of wavenumbers for which unstable linear disturbances do not grow indefinitely but achieve steady periodic waves.

5. Discussion

The present analysis predicts the existence of finite amplitude steady periodic waves. This result is in qualitative agreement with the experiments of Saric & Marshall (1971), Gold *et al.* (1971), Marshall (1971), Saric *et al.* (1973) and Gold (1973).

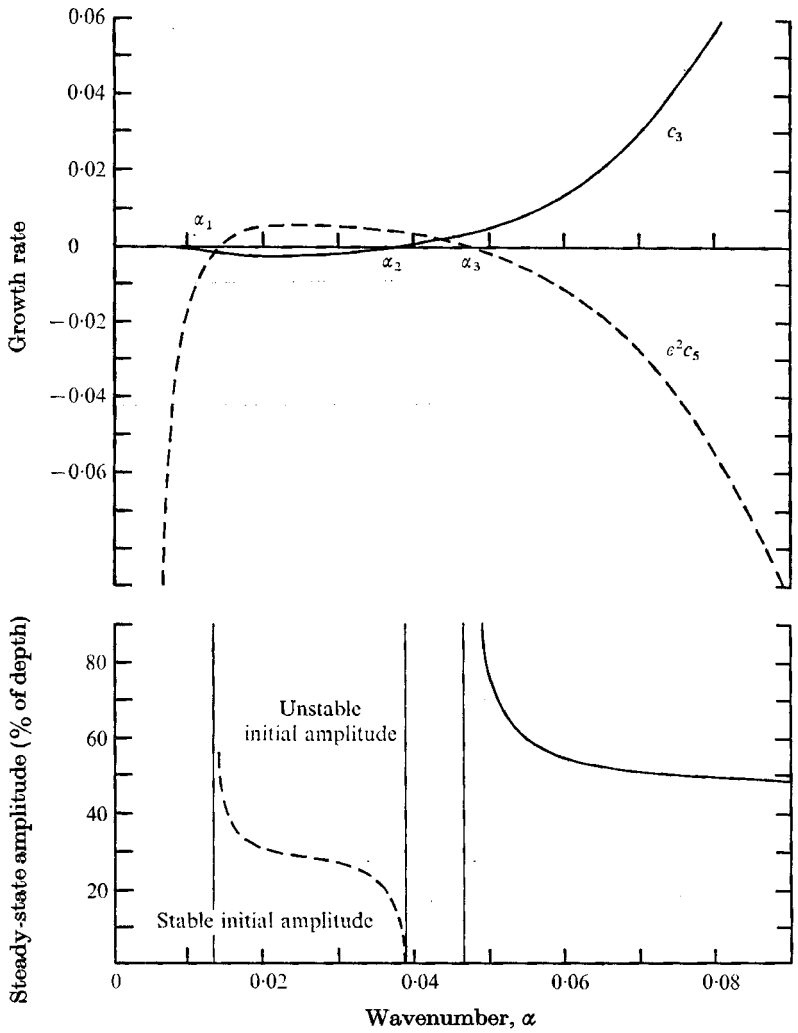

FIGURE 3. The variation of c_3 ($\epsilon^3 c_3$ is linear growth rate), c_5 ($\epsilon^5 a^2 c_5$ is nonlinear growth rate) and a_s (steady-state amplitude) with the dimensionless wavenumber α. The conditions in this case are for air over a liquid with the following characteristics: $\rho = 1{\cdot}0$ g/ml, $\nu = 0{\cdot}7$ cm^2/s, $g = -980$ cm/s^2, $\sigma = 72$ dyne/cm, $c_f(M^2-1)^{\frac{1}{2}} = 0{\cdot}003$, $M = 2{\cdot}8$, $\epsilon = 0{\cdot}5$, $R = 1{\cdot}9$, $\tau = 200$ dyne/cm^2.

In spite of the success of the present model in predicting the existence of the experimentally observed periodic waves, it cannot predict quantitatively the observed wavelength and its corresponding amplitude. Since disturbances with all wavelengths are possible in a given experiment, the observed wavelength is expected to correspond to the maximum steady-state amplitude a_s. However, figures 3 and 4 show that a_s decreases monotonically and it asymptotes to a minimum as $\alpha \to \infty$. Thus, the present model does not predict the observed wavelength because a_s does not possess a relative maximum at a finite value of α as is observed experimentally.

Figure 4 shows that, at a given wavelength, the amplitude increases with the

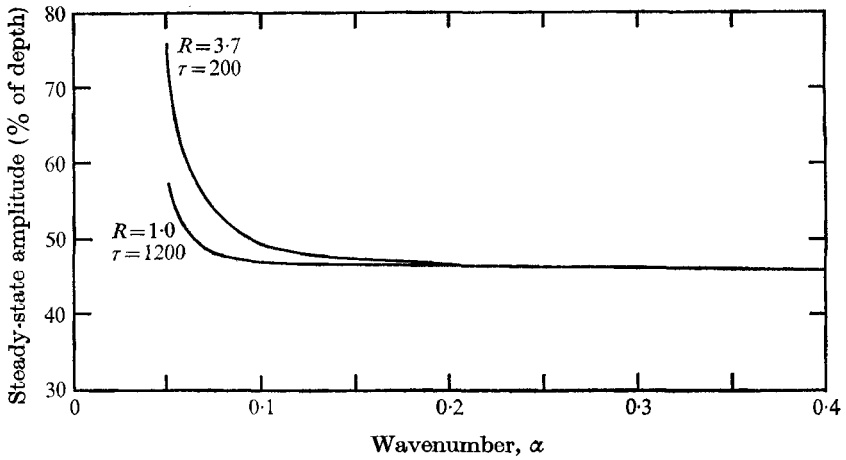

FIGURE 4. Steady-state wave amplitude as a function of shear stress and Reynolds number for the conditions of figure 3.

liquid Reynolds number R but decreases with the mean shear stress τ. For large α, a_s is independent of τ and R. The variation of a_s with R is in disagreement with the experimental observation that the ratio of the r.m.s. amplitude to the mean liquid depth decreases with increasing τ or R (Gold *et al.* 1971; Gold 1973; Saric *et al.* 1973).

The inability of the present theory to predict the observed wavelength and amplitude can be attributed to the assumptions used in calculating the stress perturbations. The disturbed gas motion was assumed to be inviscid and the gas mean velocity profile was assumed to be uniform. According to this model, the shear perturbation is neglected and the pressure perturbation is in phase with the wave slope. An order-of-magnitude analysis shows that the shear perturbation is 10 % of the pressure perturbation, and hence it can be neglected. However, including the gas viscosity (boundary sublayer) and mean velocity profile decreases the magnitude and changes the phase of the pressure perturbation, which greatly affect the stability of the interface as shown by the linear analysis of Bordner, Nayfeh & Saric (1973) and the work of Inger (1971) on cross-hatching. Thus, to predict the observed wavelength and amplitude, the present model must be modified to include the gas mean velocity profile and the gas boundary sublayer.

This work was supported by the Fluid Dynamics Program of the Office of Naval Research and the United States Atomic Energy Commission. The authors deeply appreciate the help of G. L. Bordner in checking the algebra.

Appendix

Rather than using the method of multiple scales to analyse (4.4)–(4.6), we may use the following alternative approach. We let

$$\eta_{1t} = ic_1\eta_1 + i\epsilon^2 c_2\eta_1^2\bar{\eta}_1 + \epsilon^3 c_3\eta_1 + i\epsilon^4 c_4\eta_1^3\bar{\eta}_1^2 + \epsilon^5 c_5\eta_1^2\bar{\eta}_1 + O(\epsilon^6), \qquad (A\,1)$$

$$\eta_2 = b_1\eta_1^2 + \epsilon^2 b_2\eta_1^3\bar{\eta}_1 + i\epsilon^3 b_3\eta_1^3 + O(\epsilon^4), \tag{A 2}$$

$$\eta_3 = d\eta_1^3 + O(\epsilon), \tag{A 3}$$

where $c_1 = -(1+\frac{1}{3}\chi)$. By substituting (A 1)–(A 3) into (4.4)–(4.6) and equating coefficients of equal powers of ϵ, we obtain algebraic equations for c_1, b_i and d, which can be solved in succession. The result is in full agreement with that obtained by using the method of multiple scales.

REFERENCES

BORDNER, G. L., NAYFEH, A. H. & SARIC, W. S. 1973 Stability of a liquid film adjacent to compressible streams. *Virginia Polytech. Inst. Rep.* no. E-73-3.

CHANG, I. D. & RUSSELL, P. E. 1965 Stability of a liquid adjacent to a high-speed gas stream. *Phys. Fluids*, **8**, 1018.

GATER, R. L. & L'ECUYER, M. R. 1969 A fundamental investigation of the phenomena that characterize liquid film cooling. *Purdue University Rep.* no. TM-69-1.

GOLD, H. 1973 Surface fluid and boundary layer interaction aspects of transpiration cooled nose tip concepts. *Air Force Materials Lab. Rep.* no. TR-73-8.

GOLD, H., OTIS, J. H. & SCHLIER, R. E. 1971 Surface liquid film characteristics: an experimental study. *A.I.A.A. Paper*, no. 71–623.

GRABOW, R. M. & WHITE, C. O. 1972 A surface flow approach for predicting cross-hatch patterns. *A.I.A.A. Paper*, no. 72–718.

INGER, G. R. 1971 Compressible boundary layer flow past a swept wavy wall with heat transfer and ablation. *Astronautica Acta*, **16**, 325.

MARSHALL, B. W. 1971 An experimental investigation of a liquid film on a horizontal flat plate in a supersonic gas stream. Ph.D. thesis, Oklahoma State University, Stillwater, Oklahoma.

NACHTSHEIM, P. R. 1970 Stability of cross-hatched wave patterns in thin liquid films adjacent to supersonic streams. *Phys. Fluid*, **13**, 2432.

NAYFEH, A. H. 1973 *Perturbation Methods*. Interscience.

NAYFEH, A. H. & SARIC, W. S. 1971*a* Nonlinear Kelvin–Helmholtz instability. *J. Fluid Mech.* **46**, 209.

NAYFEH, A. H & SARIC, W. S. 1971*b* Stability of a liquid film. *A.I.A.A. J.* **9**, 750.

SARIC, W. S. & MARSHALL, B. W. 1971 An experimental investigation of the stability of a thin liquid layer adjacent to a supersonic stream. *A.I.A.A. J.* **9**, 1546.

SARIC, W. S., NAYFEH, A. H. & BORDNER, G. L. 1973 Stability of liquid films interacting with supersonic streams: theory and experiment. *Sandia Lab. Res. Rep. no.* SLA-73-0165.